

# Propagation and Network Analysis for a Dipole Based Massive MIMO Antenna for 5G Base Stations

Samuelraj Chrysolite, and Anita Jones Mary Pushpa

**Abstract**—In today's fast-paced world, where everyone/everything is moving towards an online platform, the need to provide high-speed data to all is inevitable. Hence, introducing the emerging 5G technology with orthogonal frequency division multiplexing integrated with massive MIMO technology is the need of the hour. A 640 port Massive MIMO (m-MIMO) antenna with high evenly spread gain and very low delay, along with a practically possible data rate operating in the mm waveband, is proposed for a 5G base station. The individual antenna element consists of a dipole ( $\lambda=0.5\text{cm}$ ) designed to operate at 57GHz. Placing the cylindrical MIMO antenna array (8x20) facing the four directions forming the m-MIMO antenna (160x4) at the height of 3m from ground level for simulation. Achievement of a maximum gain of 23.14dBi ( $\theta=90^\circ$ ) and a minimum data rate of 1.44Gbps with -10dB bandwidth of 2.1GHz (256-QAM) approximately a distance of 478m from the 5G Base station. The m-MIMO structure gives an Envelope Correlation Coefficient of 0.015. The propagation analysis is carried out to substantiate the performance of the proposed system based on field strength and received power. Network Analysis for better reception performance is carried out by changing the antenna height placement, altering the down tilt of the antenna array, and sweeping the polarization angle of the antenna array.

**Keywords**—5G antenna; mMIMO; Dipole array; Maximum Gain

## I. INTRODUCTION

THE primary motivation behind developing a fifth-generation network (5G) is the tremendous increase in the number of users and devices connected. In order to eliminate drawbacks of the 4G LTE networks, the industries have started investing more in defining and implementing the 5G networks. It also promises to provide seamless, sustainable, and dense connectivity for further automation/intelligent gadgets development. [1] Therefore Software Defined Network is used to achieve all the performance metrics such as high network capacity (large bandwidth), dense connections (even signal strength), and efficient spectrum utilization. The architecture developed for 5G should be more flexible, reconfigurable, and scalable to reduce the cost of production for future updates. In order to produce a denser signal, millimeter waves that are above 6GHz are introduced. Qualcomm has targeted the 57GHz-66GHz (unlicensed spectrum) for 5G allocation [2]. A smaller coverage area is the backbone of 5G networks [3], which supports the concept of denser signals in order to provide an actual data rate for all users in a smaller area.

Many antenna arrays, such as hexagonal, circular, rectangular, and cross-shaped, are used in 5G systems [4]. An

array antenna system with MIMO (Multiple Input and Multiple Output) is needed to meet the complex requirements of the 5G systems. The millimeter-wave operation needs the usage of an extensive array of antennas. Usage of many antennas at the receiver side is advantageous due to increased receiver sensitivity ( $< -90\text{dBm}$ ). [5] Usage of 3D structures in the MIMO antenna reduces the space occupied and enables the 3D beamforming (omnidirectional for different planes). Performance metrics such as Gain (dBi), Half Power Beam Width (HPBW) for different " $\theta$ " and " $\phi$ " planes and channel capacity determine the efficiency of the designed array structure. For further improving the gain, signal density, channel capacity, and bandwidth, massive MIMO structures are introduced.

Massive multiple-input, multiple-output, or massive MIMO, is an extended version of MIMO, which arranges together antennas at the transmitter and receiver to improve throughput and spectrum efficiency [6]. The capability to multiply the antenna's capacity links has made m-MIMO an essential element of wireless standards, including 802.11n (Wi-Fi), 802.11ac (Wi-Fi), HSPA+, WiMAX, and LTE. Moving from MIMO to massive MIMO is shifting from using the existing radiating terminals to a large number of antennas for focusing the energy into small regions, thereby improving the throughput and efficiency of the energy radiated. Other advantages are cost-effectiveness, robustness in preventing signal jamming and simplifying the medium access layer in the network. In massive MIMO antennas, the interference between the cells reduces due to low HPBW [7]. A trade-off in the cost-effective nature of the massive MIMO antenna is that the cost of the base station will increase due to more antennas, whereas the cost will decrease in setting up the network infrastructure. Laser beams are formed due to a large number of antennas which results in high gain. The total transmits power can be reduced considerably because the transmission power for each element is scaled down to  $1/n$  ( $n$ -Total number of antenna elements). The data channel is more deterministic and reliable with many antennas as the signal is denser than the usual antennas array. The channel capacity/data rate increases linearly concerning increasing the number of antenna elements in the Massive MIMO structure [8]. The antenna geometry followed by its simulated results is shown in Section 2 A & B. The outdoor scenario is given in Section 2C, followed by the propagation and network analysis in Section 2 D & E. The work is concluded with some future works to be done in Section 3.

Samuelraj Chrysolite and Anita Jones Mary Pushpa are with Karunya University, (e-mail: [g.samuelraj@gmail.com](mailto:g.samuelraj@gmail.com), [anitajones@karunya.edu](mailto:anitajones@karunya.edu)).



## II. METHODOLOGY

### A. ANTENNA GEOMETRY-Massive MIMO(m-MIMO)

A novel dipole massive MIMO array antenna (160x4) is designed with dimensions 35x35x10cm for 5G Base station application, as shown in Fig. 1(a). The single dipole antenna is designed using (1).

$$f_r = \frac{c_0}{\lambda} \quad (1)$$

$f_r$ - Resonant Frequency,  $c_0$ - Speed of light,  $\lambda$ = wavelength of dipole(Length of the dipole). The antenna is designed for a frequency of 57GHz with a wavelength of 0.4cm.

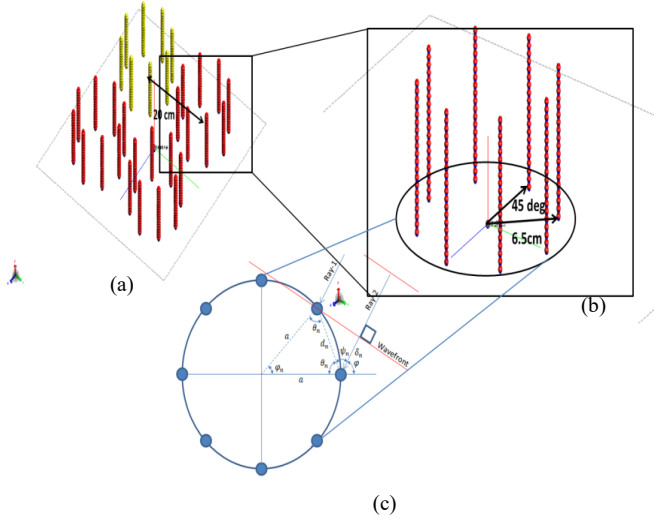


Fig. 1. M-MIMO Antenna Geometry. (a) m-MIMO Array (b) MIMO Array (c) Circular Array

The array factor for sub-array of 8 dipole elements placed in a circular format as in Figure 1(c) is calculated by (2)

$$AF = \sum_{n=0}^{N-1} e^{-jkr \cos(\varphi - \varphi_n)} \quad (2)$$

$k$ : Wave-number,  $n$ - number of elements,  $r$ - Radius of the circle defined by the circular array,  $\varphi_n$ - Direction of maximum radiation,  $\varphi$ -Angle of incidence of the plane wave. The circular antenna array with eight elements has a radius of 6.5 cm with  $\varphi_n = 45^\circ$  (equally spaced elements). The MIMO system (8x20) is designed with stacking of the circular antenna array ( $m=8$ ,  $n=20$ ) as shown in Fig. 1(b). Envelope Correlation Coefficient is an essential parameter for MIMO array antenna performance calculated by (3).

$$ECC = \frac{|S_{ii}^* S_{ij} + S_{ji}^* S_{jj}|^2}{(1 - |S_{ii}|^2 - |S_{jj}|^2)(1 - |S_{jj}|^2 - |S_{ij}|^2)} \quad (3)$$

The m-MIMO array antenna (160x4) elements are arranged in a rhombic pattern to achieve better coverage in all directions, which is desired for the base station application [9]. The distance between each array element from its center is 20cm. The arrangement can be visualized in Figure 1(a). The capacity for a Massive MIMO antenna array is calculated using (4)

$$C = MB \log_2(1 + \rho) \quad (4)$$

where  $M$ - number of antenna elements,  $B$ -Bandwidth of the Array Structure,  $\rho$ -Signal to Noise Ratio. The required design parameters for the m-MIMO array antenna are tabulated in Table I.

### B. Massive MIMO vs MIMO-A Comparative Study

#### 1. Reflection Coefficient

TABLE I  
DESIGN PARAMETERS OF M-MIMO ARRAY

Parameter	Value(cm)
Dipole Length(Single Element)	0.4
n(Number of elements in Circular Array)	8(nos)
Angle between two elements	45°
Z axis offset	0.5
Radius of Circular array	6.5
Distance between two MIMO arrays	20

In Fig. 2, for a resonant frequency of 56.9GHz, the best reflection coefficient of -43.57 dB is achieved for the MIMO system at port 100(S100,100). In comparison, the best reflection coefficient of -36dB is achieved at port 148(S148,148)for a massive MIMO array antenna with a bandwidth of 2.05GHz at -10dB substantiating the switch over from MIMO to m-MIMO array antenna. The needed bandwidth is achieved for 5G systems with more users, even though the reflection coefficient is compromised

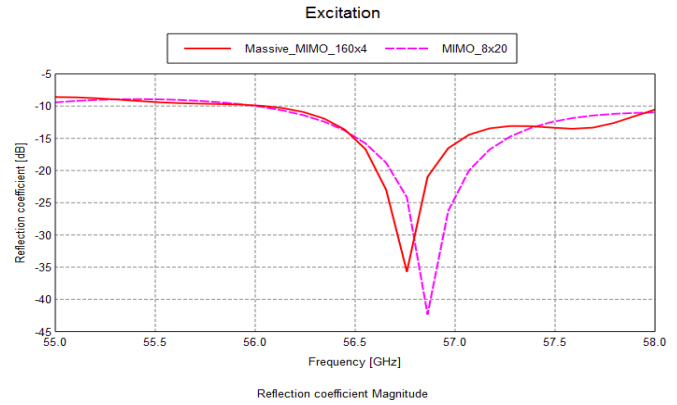


Fig. 2. Reflection Coefficient

#### 2. Voltage Standing Wave Ratio

The Voltage Standing Wave Ratio at 56.9 GHz is 1.1 for MIMO array antennas. At the same time, a VSWR of 1.2 is achieved for the m-MIMO array antennas, which suggests that the standing waves are very low, enabling maximum radiation, as shown in Fig. 3. It avoids the cancellation of the electromagnetic waves traveling through the antenna structure, thereby resulting in good radiation.

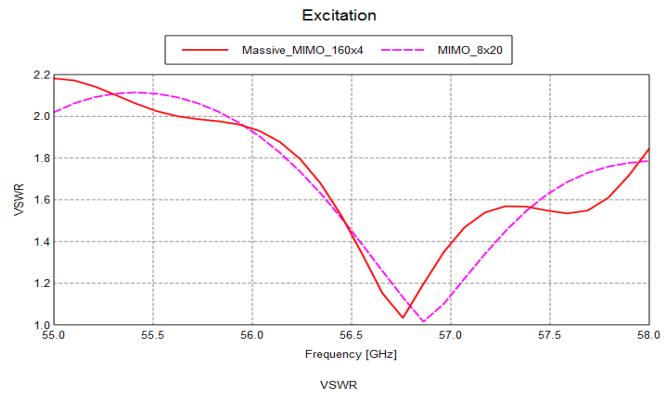


Fig. 3. Voltage Standing Wave Ratio

### 3. Far-Field Analysis

The far-field around the m-MIMO array antenna proposed is validated by the polar plot for Gain(dBi) and the radiation pattern(3D). The main advantage of switching from MIMO to m-MIMO is the notable improvement in gain and reduction in half-power beam width (HPBW), thereby improving the directivity.

#### i. Gain (2-Dimensional)

A comparative polar plot for the far-field is given in Fig. 4. A maximum gain of 23dBi is achieved at  $\theta=90^\circ, \phi=10^\circ$  for MIMO array antenna while an improved 26.6dBi is achieved at  $\theta=90^\circ, \phi=55^\circ$  for the m-MIMO array antenna. Moreover, the HPBW for the MIMO system is measured as  $3.5^\circ$ , which further reduces to  $2.1^\circ$  for Massive MIMO, thereby improving isolation of those laser beams (interference mitigation).

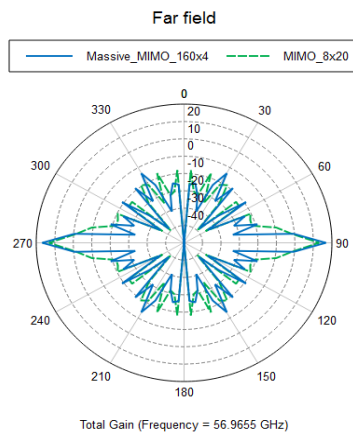


Fig. 4. Gain(Far-Field)

#### ii. 3-D Pattern

The same far-field gain is plotted for MIMO and m-MIMO on a 3-D view, as shown in Fig. 5(a), Fig. 5 (b). The beams become thinner when the number of antenna elements increases in the m-MIMO array antenna reducing the interference between two beams in the array structure. Moreover, the Half power Null Width (HPNW) reduces from  $15^\circ$  to  $10^\circ$  increasing the spatial density of the radiating signal in the far-field without interference.

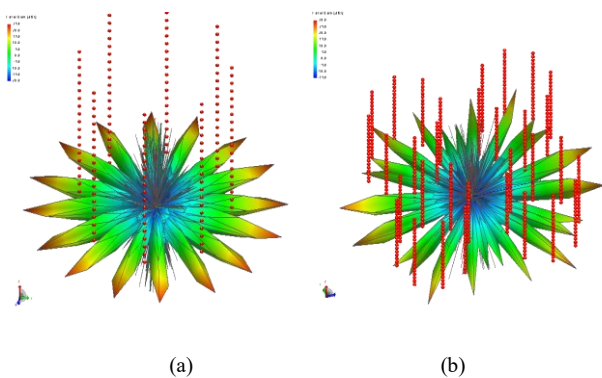


Fig. 5. 3-D Radiation Pattern (Gain-Far-Field) (a) MIMO (b) m-MIMO

### 4. Comparison Inference

When the MIMO array antenna is converted into an m-MIMO array antenna, the antenna gain increases from 23dBi to 26.6dBi. Moreover, the bandwidth which determines the capacity increases from 1.5 GHz to 2.05GHz. The Half power beamwidth also decreases from  $3.5^\circ$  to  $2.1^\circ$ . The proposed m-MIMO antenna array outperforms the various m-MIMO antenna array proposed by various researchers and authors in terms of Bandwidth, Gain, Half Power Beam Width, Half Power Null Width, as shown in Table II. The m-MIMO antenna array (5G base station) with a bandwidth of 2.05GHz, a gain of 26.6dBi, and a HPBW of 2.1 degrees are considered for the propagation and network analysis.

TABLE II  
PERFORMANCE ANALYSIS

Ref	Array Config.	Resonant Frequency	Reflection Coefficient	Bandwidth (-10dB)	VSWR	Gain	HPBW	HPNW
[10]	32x3	2.6GHz	-21dB	300 MHz	1.8	3dBi	53°	5°
[11]	6x2	3.6GHz	-35dB	400 MHz	1.6	2.1dBi	65°	10°
[12]	16x16	5.6GHz	-32dB	1GHz	1.45	17.4dBi	42°	12°
[13]	96x3	3.5GHz	-30dB	100MHz	1.2	19.5dBi	28°	5°
[14]	4x4	3.6GHz	-28dB	1.2GHz	1.17	6.78dBi	29.3°	18.3°
<b>This work</b>	<b>160x4</b>	<b>5.7GHz</b>	<b>-36dB</b>	<b>2.05 GHz</b>	<b>1.2</b>	<b>26.6dBi</b>	<b>2.1°</b>	<b>10°</b>

### C. OUTDOOR SCENARIO

The proposed massive MIMO antenna for the 5G Base station is verified by downloading an outdoor scenario consisting of various buildings (densely populated), bridges, tunnels, etc., via ALTAIR (Proman) using open street view maps online. The buildings are defined from a materialistic perspective with different architectures, heights, and interiors. A prediction area of 2km x 1 km from Munich (Germany) is considered due to its high density of buildings. The material characteristics are kept to default (concrete). The schematic layout of the considered layout with the base station placed at the center is shown in Fig. 6(a), Fig. 6(b).

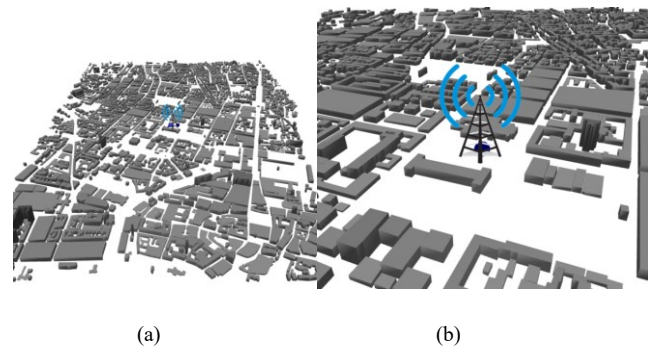


Fig. 6 Outdoor scenario of 3km x 2km area in Munich, Germany (a) Outdoor Scenario (Munich, Germany) (b) Scenario with Base station (Zoomed View)

For the propagation and network analysis, the proposed m-MIMO antenna is placed over a base station mast. The placement of the entire setup is checked for its viability in the aforementioned densely populated scenario (Munich, Germany). The measurement is done by considering a propagation path that passes through the tall buildings to better predict the field strength in the scenario considered.

#### D. PROPAGATION ANALYSIS OF *m*-MIMO IN PROPOSED SCENARIO

Various aspects such as Field strength, Received Power, Line of Sight, and Path Loss are measured for the above scenario shown in Figure 5. A presentation plot is shown for the propagation parameters.

##### 1. Field Strength

The field strength measured in dB  $\mu\text{V}/\text{m}$  is calculated using (5) and plotted on a 3D surface, indicating the strength of the electric field at various places of the considered scenario, as shown in Fig. 7. A field strength of  $> 100$  dB  $\mu\text{V}/\text{m}$  (orange color) is achieved within the 500m range from the transmitter.

$$E = \frac{\sqrt{30GP}}{R} \quad (5)$$

Where G- Antenna Gain(dBi), P- Transmitter Power(Watts), R- Distance between the sensor and the antenna

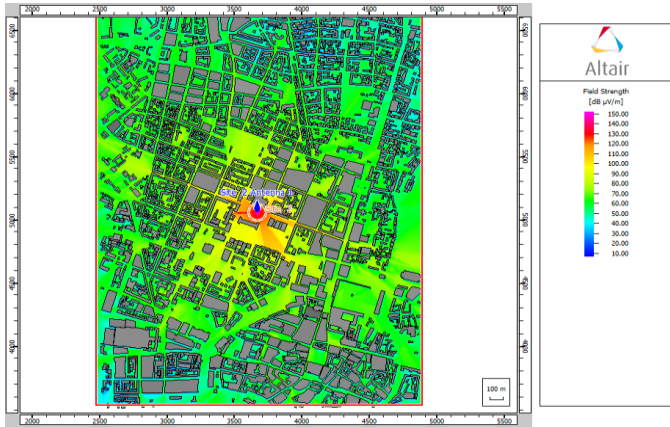


Fig. 7. Field strength of the proposed *m*-MIMO antenna (Munich, Germany)

##### 2. Received Power

The average receiver sensitivity measured in dBm according to (6) is -90dBm [10]. Therefore the received power is plotted on a 3D surface, indicating the power received at various places of the considered scenario, as shown in Fig. 8.

$$S = 10 \log KTB + NF + SNR \quad (6)$$

S- receiver sensitivity, in dBm, k- Boltzmann constant, in J/K, T- absolute temperature, in K, B: signal bandwidth, in Hz, kTB- thermal noise power within the bandwidth range, in Watts, NF: noise factor, in dB, SNR: signal-to-noise ratio in dB.

The surface graph is plotted so that the places that receive the power of greater than -90dBm (standard receiver sensitivity) are marked in red, and the other areas are marked in green. The area shown in red covers approximately 489m from the massive MIMO array antenna (5G Base station).

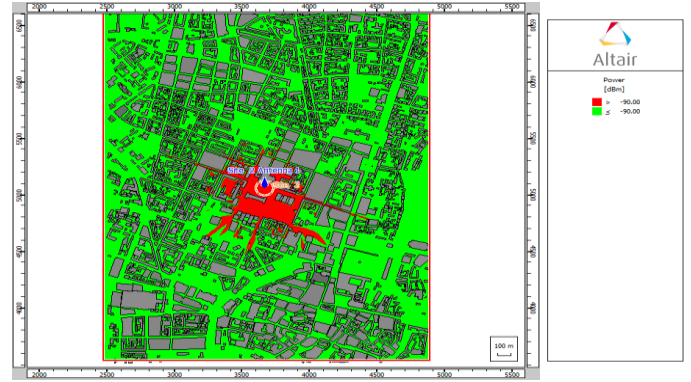


Fig. 8. Received power of the proposed *m*-MIMO antenna (Munich, Germany)

##### 3. Line of Sight (LOS)

The Line of Sight area for the proposed 5G base station has been marked green, indicating the area of direct contact of the radiated signal in the considered scenario, as shown in Fig. 9. As the outdoor scenario is considered, the other areas fall under the Non-Line of Sight (NLOS) region.

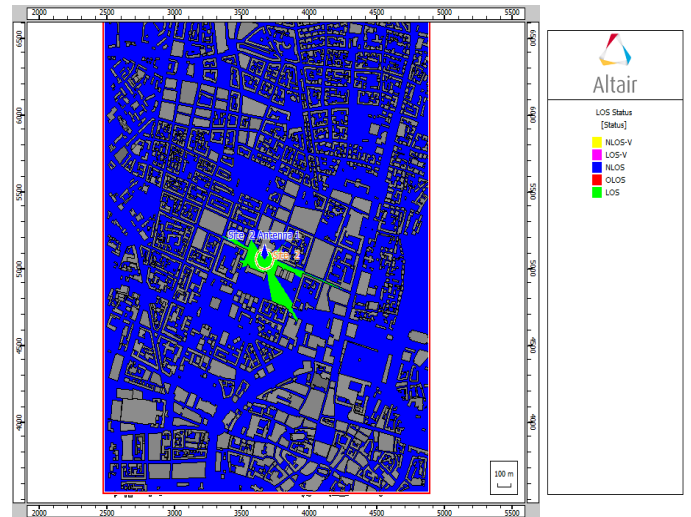


Fig. 9. Line of Sight for the proposed *m*-MIMO antenna (Munich, Germany)

##### 4. Path Loss

The maximum path loss for efficient signal transmission is calculated by (7). The path loss measured in dB is less than -144db within the 500m radius from the transmitter antenna, which is the maximum allowed path loss [15]. The path loss is more in areas with dense buildings, as shown in Fig. 10.

$$MPL = P_{Tx} + Gain_{Tx} + Gain_{Rx} + S \quad (7)$$

where MPL-Maximum Path Loss,  $P_{Tx}$ -Transmitter Power,  $Gain_{Tx}$ -Transmitter Gain,  $Gain_{Rx}$ -Receiver Gain, S – Receiver Sensitivity.

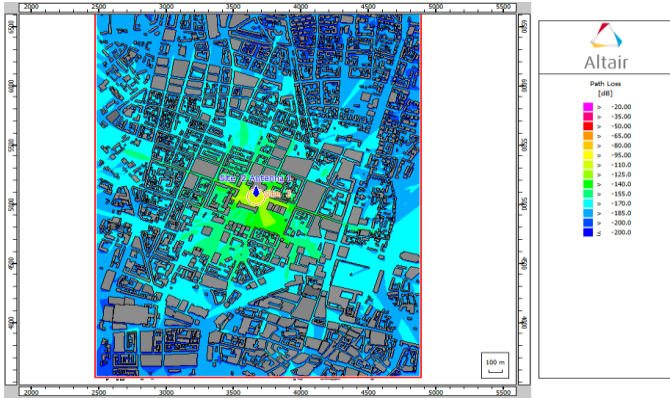


Fig. 10. Path loss for the proposed m-MIMO antenna (Munich, Germany)

### E. NETWORK ANALYSIS

The network formed through the proposed 5G Base station antenna is analyzed for compatibility, cost-effectiveness, robustness, effective data rate, and overall efficiency. Some of the network parameters considered for the analysis are Multiple Access techniques, Traffic Types, Duplex separation types, number of MIMO streams, Channel Bandwidth, Modulation techniques, Code rate, and the number of resource blocks used for both uplink and downlink cases. The various parameters considered for the below network analysis are tabulated in Table III. Based on the below parameters, the network is analyzed for the following sub-headings. The network scenario and the receiver antenna (User Equipment) are shown in Fig. 11.

TABLE III  
NETWORK PARAMETERS OF MASSIVE MIMO

Multiple Access Technique	OFDM / SOFDMA[16]
Traffic	Homogenous and Static
Duplex Separation	Time Division Duplexing[17]
MIMO streams	4 [18]
Channel Bandwidth	2.1 GHz
Modulation Technique	1024-QAM [19]
Code Rate	3/3 (Ratio-1)
Resource blocks	2 (Minimum)
Resolution	2.5m

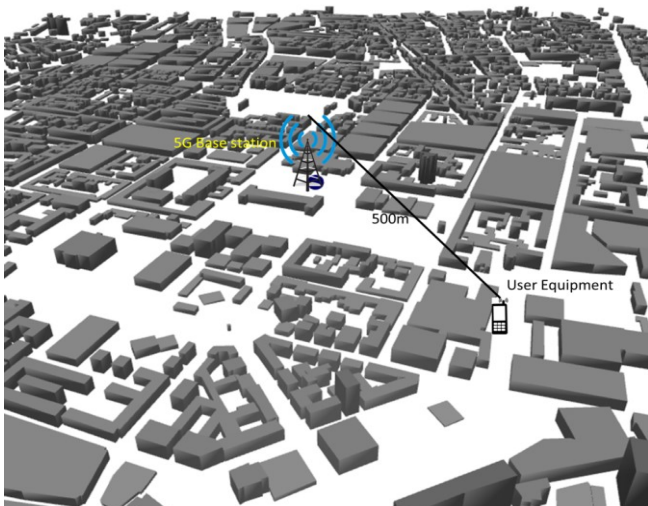


Fig. 11. Network Scenario with Transmitter and Receiver

### 1. HEIGHT OF ANTENNA PLACEMENT

The received power is plotted for various heights of antenna placement at the receiver antenna (User Equipment) placed at a 500 m distance from the transmitter. Lower height levels are considered for 5G base stations to reduce the area of the no-signal region right below the base station mast. The massive MIMO array antenna performs better at the height of 3m, providing better-received power within the 500m regions, as shown in Fig. 12.

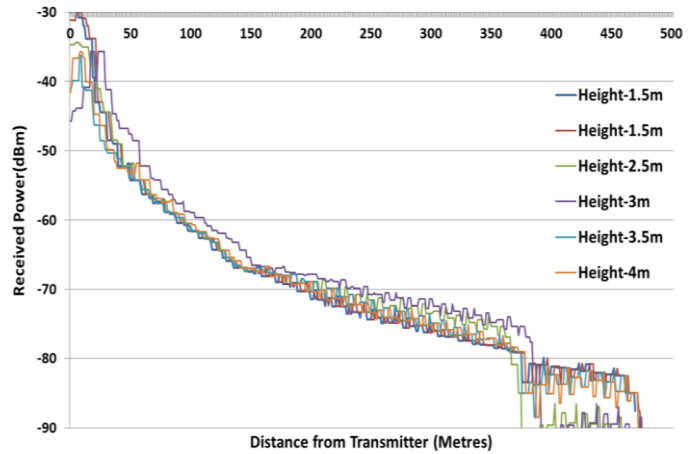


Fig. 12. Received power for various Base station mast height

### 2. Down Tilt of the Antenna

The received power is plotted for various outward down tilt angles of the proposed antenna, as illustrated in Fig. 13. A denser signal is achieved inside the 500m region, and the no-signal area below the transmitter is further reduced. The massive MIMO array antenna performs better at a down tilt angle of 45 degrees, as shown in Fig. 14, providing better-received power within the 500m region. At a 45 degree angle, intrusion of the beam inside the buildings is much better than the performance with other angles of tilts.

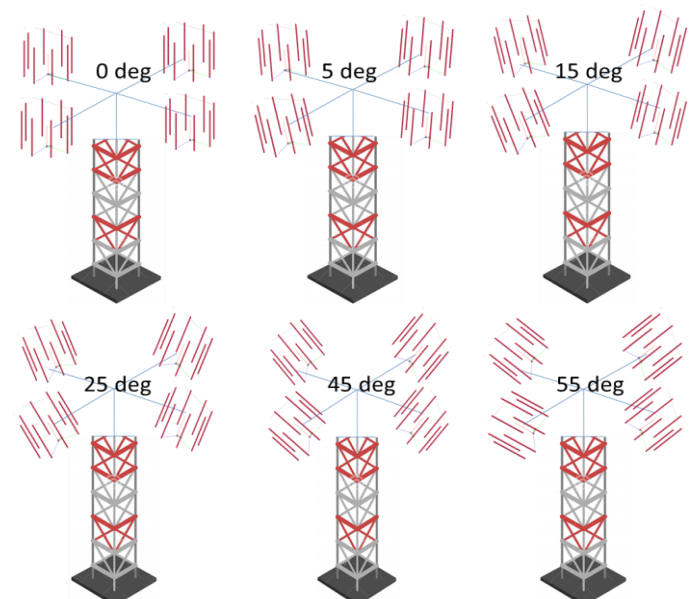


Fig. 13. Illustration of various down tilt angle of the proposed antenna

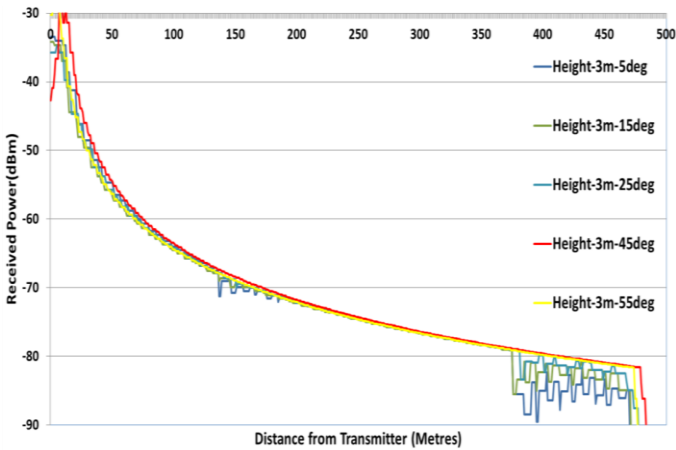


Fig. 14. Received power for various down tilt angle (outward)

### 3. Transmission Power

The received power is plotted for various transmission powers at the transmitter is shown in Fig. 15. The transmission power of 10 W (40dBm) provides the necessary received power (>-90dBm) [15] within the 500m range [20] for the efficient performance of the proposed massive MIMO array. The comparative study given in Figure 14 suggests that 5G Base stations can very well work with low transmission powers.

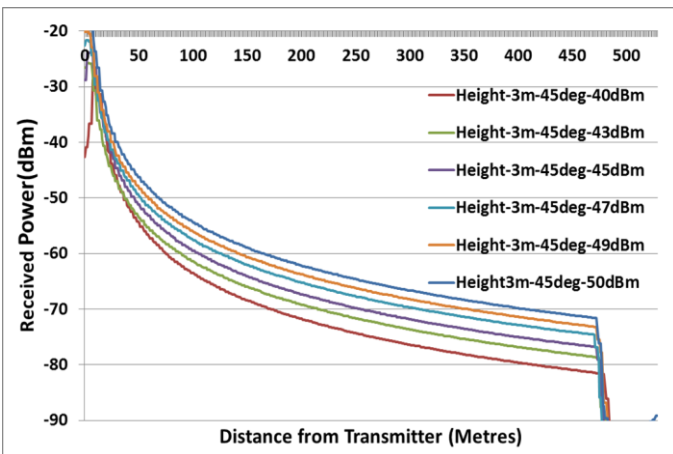


Fig. 15. Received power for various transmission powers

### 4. Transmission Modes

The various modulation techniques are used to achieve a better data rate/channel capacity for the data transmission from the transmitter (Downlink) and the data reception at the same base station (Uplink). The Quadrature Amplitude Modulation (QAM) is considered for the analysis as it is used to increase the channel bandwidth and thereby increase the data rate in the considered 5g scenario [19]. Various types of QAM are implemented, and the data rates [8] are plotted as shown in Fig. 16. The 1024-QAM proves to be the best based on the data rate provided, and a theoretical data rate of 11Gb/sec can be achieved when a maximum number of resource blocks are used (max-16).[21]

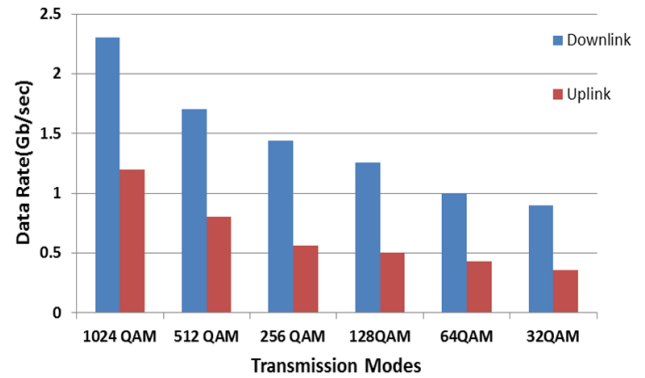


Fig. 16. Data Rates for different QAM (Uplink and Downlink)

### 5. Polarization

The received power is plotted for various linear polarization angles for the input signal at the transmitter, as shown in Fig. 17. An angle of 45 degrees provides more intrusion into the buildings maintaining the received power inside the buildings instead of an exponential drop of 5-8dBm.

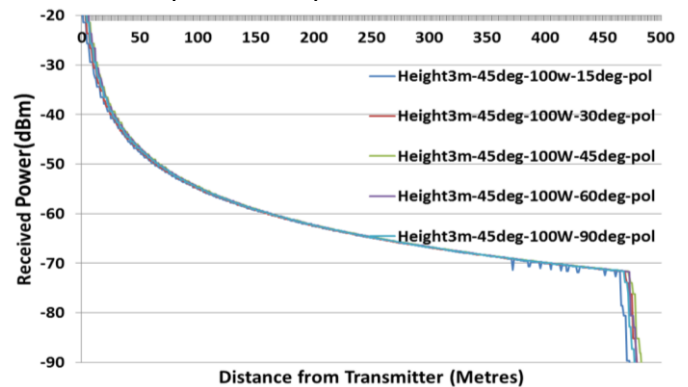


Fig. 17. Received power for Linear polarization angles

### 6. Heights of Reception

To check whether the signal reception is even at all levels of the considered scenario, the received power is plotted for various prediction planes such as human height, bus, bridges, and multi-storeyed buildings, as shown in Fig. 18. It is inferred that the signal level (Received Power) is even when we travel by foot (Height=1.8m) or when we travel by bus (Height=1.8m) or when we are on a bridge (Height= 3m) or when we are in a multi-storey building (Height ≥ 4m).

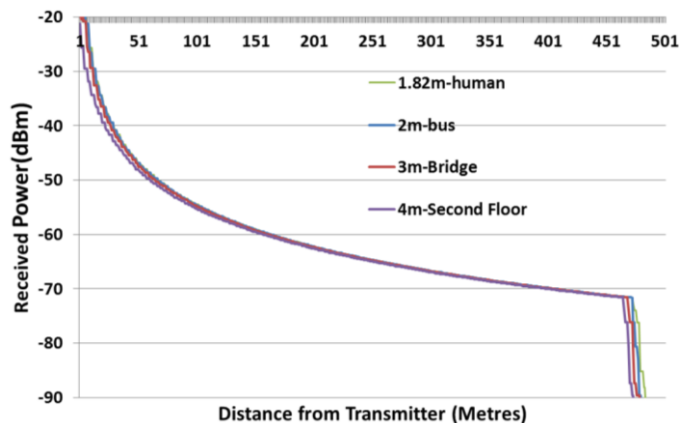


Fig. 18. Received power for various polarization angles

## CONCLUSION

The proposed dipole-based m-MIMO antenna array for 5G base station performs well in aspects such as Gain, Directivity, Transmission Power, Transmission Range, Capacity /Data Rate. The 5G platform aims to provide society with a seamless data environment that fulfills the aspects mentioned above. Further investigations can be carried out on the overall placement of each antenna element in the m-MIMO antenna array (Non-Linear array) to avoid the wastage of power in directions that are not intended or to tap energy from unavoidable side beams dissipated from the m-MIMO antenna array. The propagation and network analysis can be done with vegetation and different types of scattering. The Monte-Carlo simulation can also find out the best and worst-case scenarios at different traffic conditions.

## REFERENCES

- [1] Luo, Wei, et al. "A Low-Profile Dual-Band Base Station Antenna with Antenna on Antenna Structure." *Progress In Electromagnetics Research*, vol. 109 (2021): 77-94. <https://doi.org/10.2528/PIERC20110102>
- [2] <https://www.qualcomm.com/media/documents/files/spectrum-for-4g-and-5g.pdf>
- [3] Al-Falahy, Naser, and Omar Y. Alani, "Technologies for 5G networks: Challenges and opportunities." *IT Professional* 19.1 (2017): 12-20. <https://doi.org/10.1109/MITP.2017.9>
- [4] Zhang, Jing, et al. "5G millimeter-wave antenna array: Design and challenges," *IEEE Wireless communications* 24.2 (2016): 106-112. <https://doi.org/10.1109/MWC.2016.1400374RP>
- [5] Huo, Yiming, Xiaodai Dong, and Wei Xu. "5G cellular user equipment: From theory to practical hardware design," *IEEE Access* vol. 5 (2017): 13992-14010. <https://doi.org/10.1109/ACCESS.2017.2727550>
- [6] Marzetta, and Thomas L. "Massive MIMO: an introduction," *Bell Labs Technical Journal* 20 (2015): 11-22. <https://doi.org/10.15325/BLTJ.2015.2407793>
- [7] Marzetta, Thomas L. "Fundamentals of massive MIMO," *Cambridge University Press*, 2016. <https://doi.org/10.1017/CBO9781316799895>
- [8] Björnson Emil, Jakob Hoydis, and Luca Sanguinetti. "Massive MIMO has unlimited capacity," *IEEE Transactions on Wireless Communications* 17.1 (2017): 574-590. <https://doi.org/10.1109/TWC.2017.2768423>
- [9] Honda, Kazuhiro, Taiki Fukushima, and Koichi Ogawa. "Full-Azimuth Beam Steering MIMO Antenna Arranged in a Daisy Chain Array Structure," *Micromachines* 11.9 (2020): 871. <https://doi.org/10.3390/mi11090871>
- [10] Chen, Cheng-Ming, et al. "Finite large antenna arrays for massive MIMO: Characterization and system impact," *IEEE Transactions on Antennas and Propagation* 65.12 (2017): 6712-6720. <https://doi.org/10.1109/TAP.2017.2754444>
- [11] Li, Yixin, Yong Luo, and Guangli Yang. "12-port 5G massive MIMO antenna array in sub-6GHz mobile handset for LTE bands 42/43/46 applications," *IEEE access* 6 (2017): 344-354 <https://doi.org/10.1109/ACCESS.2017.2763161>
- [12] Komandla, Mohana Vamshi, Ghanshyam Mishra, and Satish K. Sharma, "Investigations on dual slant polarized cavity-backed massive MIMO antenna panel with beamforming," *IEEE Transactions on Antennas and Propagation* 65.12 (2017): 6794-6799. <https://doi.org/10.1109/TAP.2017.2748239>
- [13] <https://doi.org/10.1109/TAP.2017.2748239>
- [14] Al-Tarifi, Monjed A., Mohammad S. Sharawi, and Atif Shamim. "Massive MIMO antenna system for 5G base stations with directive ports and switched beamsteering capabilities," *IET Microwaves, Antennas & Propagation* 12.10 (2018): 1709-1718. <http://dx.doi.org/10.1049/iet-map.2018.0005>
- [15] Pfadler, Andreas, et al. "Multi-antenna configuration modeling for massive MIMO V2I." (2018): 729-5 <https://doi.org/10.1049/cp.2018.1088>
- [16] <https://www.qualcomm.com/media/documents/files/deploying-5g-nr-mmwave-for-indoor-outdoor.pdf>
- [17] Ndovi, Lusungu, Charles S. Lubobya, and Ackim Zulu, "Beamforming for 5G mm Wave Networks at Quadrature Baseband and RF using OFDM signaling," *International Journal of Innovative Science and Research Technology* Volume 6, Issue 2, February – 2021 ISSN No:-2456-2165.
- [18] Jaewon Lee, Minjoong Rim, and Chung G. Kang, "Decentralized Slot-ordered Cross Link Interference Control Scheme for Dynamic Time Division Duplexing (TDD) in 5G Cellular System," *IEEE Access* (2021). <https://doi.org/10.1109/ACCESS.2021.3074176>
- [19] Liu Xin, et al. "Multi-Stream Spatial Digital Predistortion for Fully-Connected Hybrid Beamforming Massive MIMO Transmitters," *IEEE Transactions on Circuits and Systems I: Regular Papers* (2021). <https://doi.org/10.1109/TCSI.2021.3072591>
- [20] Wang, Yanyi, et al. "QAM vector mm-wave signal generation based on optical orthogonal polarization SSB scheme by a single modulator," *Journal of Lightwave Technology* (2021). <https://doi.org/10.1109/JLT.2021.3068742>
- [21] Eid, Aline, Jimmy GD Hester, and Manos M. Tentzeris, "5G as a wireless power grid," *Scientific Reports* 11.1 (2021): 1-9. <https://doi.org/10.1038/s41598-020-79500-x>
- [22] Marwat, Safdar Nawaz Khan, et al. "Method for handling massive IoT traffic in 5G networks," *Sensors* 18.11 (2018): 3966. <https://doi.org/10.3390/s18113966>